NUMERICAL MODELING OF OPTICAL PROPERTIES OF CLOUD PARTICLES OF COMPLEX COMPOSITION

L.S. Ivlev, K.Ya. Kondrat'ev, and O.M. Korostina

State University, St. Petersburg
Scientific–Research Center for Ecological Safety, St. Petersburg
Received July 23, 1992

Some results of numerical simulations of optical characteristics of light scattering by polydisperse systems of uniform and two–layer spherical particles are presented. These characteristics are a set of modes corresponding to particles of different origin.

When investigating the cloud formations it was experimentally shown that liquid cloud elements contain, in addition to water, other substances in both dissolved and solid states. However, the distribution of the undissolved substance inside a droplet or in its external cover is unknown. A solid cover of particles, or tar–like shields of droplets, as well as the ice layered particles are observed in some cases. At the same time, a portion of fine particles exists inside a cloud for quite a long time without merging into droplets.

Since it is too difficult technically to classify different types of distributions of a disperse substance based on observational data, numerical modeling of optical characteristics becomes important, and, in particular, it can be of certain interest for verification of different optical methods of identification of the microstructure of clouds and other aerosol formations.

Optical properties of small particles are determined, first of all, by their cover. Therefore, models of spherical particles, which can be described taking into account some principal particle types such as homogeneous and multilayer spheres, spheres with microparticles disseminated inside them which strongly absorb radiation, and the mixture of particles with different optical constants, are quite adequate.

The third aerosol type can be approximately reduced to the first but with imaginary part of the complex refractive index greater than that of the basic substance of the sphere with disseminations. The multilayer spheres can be approximated by the double–layer ones, as it follows from the papers by A.P. Prishivalko et al.[1–3]

Generally speaking, the admissibility of the change of a conglomerate particle composed of microparticles with different complex refractive indices should be varified. However, the available results[4–5] make it possible to think that this assumption is valid to a high degree of accuracy. Then it follows that for great values of relative humidity (for the majority of particles up to $f \simeq 90$–95% and in some cases up to $f \simeq 75$–80%) the assumption that water is uniformly mixed with other compounds comprising the substance of particles is valid.

Let us now discuss the results of numerical modeling of the effect of particles inhomogeneity on the aerosol optical parameters for the polydisperse models A and B consisting of several modes (fractions). All the modes are described by the same type of the particle size distribution function

$$dN_i/dr = N_{0i}\, r^{-6}\, e^{-6r_{0i}/r}\,, \qquad (1)$$

where N_{0i} is the number density, r_{0i} is the modal radius which correspond to the following modes:

Mode I. Condensation nuclei (new particles of the condensation origin): $r_{01} = 0.026$ μm, $r_{\min} = 0.0026$ μm, $r_{\max} = 0.13$ μm, and $N_{01} = 10^4$.

Mode II. Very old particles: $r_{02} = 0.14$ μm, $r_{\min} = 0.014$ μm, $r_{\max} = 0.7$ μm, and $N_{02} = 10^3$.

Mode III. The products of chemical and photochemical reactions in a polluted atmosphere: $r_{03} = 0.22$ μm, $r_{\min} = 0.022$ μm, $r_{\max} = 1.1$ μm, and $N_{03} = 10^2$.

Mode IV. $r_{04} = 0.45$ μm, $r_{\min} = 0.045$ μm, $r_{\max} = 2.25$ μm, and $N_{04} = 10^1$.

Mode V. Disperse particles of the erosion origin: $r_{05} = 2$ μm, $r_{\min} = 0.2$ μm, $r_{\max} = 10$ μm, and $N_{05} = 10^0 = 1$.

Polydisperse systems of aerosol particles were represented by homogeneous and double–layer spheres. The cover was 0.1, 1, and 10% of the total mass of the sphere. The refractive indices of the substances of cover and core varied.

In the case of homogeneous particles we used the model from Ref. 6 as the A model with complex refractive indices of particles substance $\tilde{m} = (\tilde{n} - i\tilde{k})$ of different modes being assigned assuming uniform distribution of different substances, and also assuming that the absorption $\tilde{k}$ is due to the presence of soot. The values $\tilde{n}$ and $\tilde{k}$ are shown in Table I. In the case of double–layer particles the core is composed of the substances of model aerosols without absorption $\tilde{m}_c = (\tilde{n} - i0)$, and the shield is of soot with complex refractive index $m_{sh} = (n - i\kappa)$. The model B describes a system of homogeneous water droplets or of soot particles and double–layer particles covered with the soot shield.

The energy characteristics (extinction coefficient σ_{ext}, scattering coefficient σ_{sc} and the absorption coefficient σ_{abs}) and angular characteristics (scattering phase function $I(\theta)$, asymmetry coefficient Γ, and degree of linear polarization $P(\theta)$) were considered (Tables II–V).

0235-6880/92/11 770-08 $02.00

TABLE I. The "effective" complex refractive index $\tilde{m} = (\tilde{n} - i\tilde{k})$ for the model A.

λ, μm	Modes									
	1		2		3		4		5	
	$\tilde{n}$	$\tilde{k}$	$\tilde{n}$	$\tilde{k}$	$\tilde{n}$	$\tilde{k}$	$\tilde{n}$	$\tilde{k}$	$\tilde{n}$	$\tilde{k}$
0.32	1.486	0.075	1.52	0.075	1.538	0.05	1.538	0.0226	1.556	0.0091
0.40	1.47	0.075	1.52	0.075	1.53	0.05	1.53	0.021	1.54	0.007
0.55	1.47	0.0745	1.52	0.07475	1.53	0.05	1.53	0.021	1.53975	0.00375
0.65		0.0735	1.52	0.07425	1.53	0.05	1.53	0.021	1.53925	0.00325
1.03	1.47	0.06961	1.54871	0.071129	1.5439	0.04761	1.54	0.02061	1.53761	0.003
1.40	1.4739	0.0684	1.566	0.0694	1.556	0.047	1.546	0.01866	1.535	0.003
2.40	1.48	0.0745	1.5375	0.0735	1.5225	0.04835	1.51	0.02675	1.5005	0.00675
	1.48									

TABLE II. The ratio of the absorption efficiencies σ_{abs} (double–layer)/σ_{abs} (homogeneous). Model A: homogeneous particle $m = \tilde{m} = (\tilde{n} - i\tilde{k})$, double–layer: soot cover, core $\tilde{m}$ without absorption.

λ, μm	Modes											
	1		2		3		4			5		
	Soot, %											
	10	1	10	1	10	1	10	1	0.1	10	1	0.1
0.32	0.86	0.1	0.74	0.16	0.81	0.21	0.97	0.34	0.05	0.97	0.6	0.13
0.4	0.87	0.1	0.75	0.14	0.84	0.2	1.04	0.34	0.05	1.12	0.65	0.14
0.55	0.89	0.1	0.77	0.13	0.89	0.18	1.16	0.34	0.045	1.74	0.89	0.17
0.65	0.9	0.1	0.79	0.12	0.92	0.17	1.22	0.33	0.044	2.09	0.92	0.186
1.03	0.92	0.1	0.82	0.1	1.02	0.15	1.46	0.31	0.037	2.86	1.14	0.182
1.4	0.93	0.1	0.84	0.1	1.09	0.15	1.79	0.33	0.037	3.39	1.21	0.187
2.4	0.89	0.1	0.87	0.1	1.23	0.14	1.77	0.25	0.027	2.46	0.74	0.100

TABLE III. The ratio of the absorption efficiencies σ_{abs} (double–layer)/σ_{abs} (homogeneous). Model B: double–layer particle is water + soot 10, 1 0.1%, homogeneous particle is soot.

λ, μm	Modes											
	1		2		3		4			5		
	Soot, %											
	10	1	10	1	10	1	10	1	0.1	10	1	0.1
0.32	0.17	0.016	0.6	0.12	0.7	0.19	0.85	0.32	0.05	0.98	0.64	0.15
0.4	0.15	0.016	0.52	0.09	0.66	0.15	0.81	0.28	0.04	0.98	0.61	0.13
0.55	0.14	0.014	0.42	0.06	0.57	0.11	0.75	0.22	0.03	0.97	0.53	0.11
0.65	0.14	0.014	0.37	0.05	0.51	0.09	0.71	0.19	0.02	0.95	0.49	0.09
1.03	0.15	0.015	0.25	0.03	0.36	0.05	0.58	0.12	0.013	0.88	0.38	0.06
1.4	0.16	0.018	0.2	0.02	0.28	0.03	0.48	0.09	0.017	0.83	0.35	0.095
2.4	0.19	0.02	0.16	0.02	0.2	0.02	0.34	0.05	0.01	0.78	0.26	0.06

TABLE IV. Assymetry of the scattering phase function Γ. Model A: double–layer: $\tilde{m}$ without absorption + soot (10 and 1%), homogeneous $\tilde{m}$.

λ, μm	Modes															
	1			2			3			4				5		
	Homo–geneous	Double–layer		Homo–geneous	Double–layer		Homo–geneous	Double–layer		Homo–geneous	Double–layer			Homo–geneous	Double–layer	
		10 %	1 %		10 %	1 %		10 %	1 %		10 %	1 %	0.1 %		10 %	1 %	0.1 %
0.32	0.37	0.38	0.36	2.20	1.80	1.30	2.97	2.37	1.50	4.51	4.07	2.30	1.90	50.00	58.3	17.9	–
0.4	0.28	0.28	0.28	1.80	1.50	1.20	2.31	2.04	1.38	3.35	3.49	2.05	1.74	21.80	25.9	11.7	7.7
0.55	0.19	0.19	1.19	1.30	1.20	1.02	1.73	1.65	1.24	2.35	2.71	1.68	1.48	7.02	13.8	6.4	4.5
0.65	0.16	0.16	0.16	1.15	1.11	0.98	1.50	1.47	1.15	2.01	2.38	1.53	1.37	4.90	10.2	4.8	3.6
1.03	0.12	0.12	0.12	0.72	0.73	0.69	1.03	1.03	0.92	1.44	1.68	1.24	1.16	2.70	5.2	2.8	2.3
1.4	0.11	0.11	0.11	0.48	0.49	0.47	0.81	0.93	0.78	1.17	1.35	1.08	1.04	2.10	3.9	2.3	1.9
2.4	0.10	0.10	0.11	0.25	0.25	0.25	0.43	0.45	0.43	0.98	1.02	0.95	0.93	1.80	2.7	1.7	1.5

TABLE V. Assymetry of the scattering phase function Γ. *Model B: double–layer particle is water + soot* (10, 1, *and* 0.1%), *homogeneous water, homogeneous soot.*

λ, μm	Modes																				
	1				2				3				4					5			
	Homo–geneous		Double–layer		Homo–geneous		Double–layer		Homo–geneous		Double–layer		Homo–geneous		Double–layer			Homo–geneous		Double–layer	
	H_2O	Soot	10 %	1 %	H_2O	Soot	10 %	1 %	H_2O	Soot	10 %	1 %	H_2O	Soot	10 %	1 %	0.1 %	H_2O	Soot	10 %	1 %	0.1 %
0.32	0.36	0.31	0.38	0.37	2.13	3.00	2.80	2.30	2.20	4.60	3.40	2.50	2.43	6.35	4.36	3.06	2.53	14.40	38.6	38.4	22.90	16.40
0.40	0.27	0.25	0.28	0.27	2.06	2.30	2.50	2.20	2.22	3.84	3.10	2.46	2.27	5.87	3.88	2.76	2.33	13.20	20.6	26.8	15.60	18.20
0.55	0.18	0.18	0.19	0.18	1.82	1.44	1.99	1.87	2.15	2.69	2.68	2.29	2.23	5.04	3.49	2.59	2.27	5.89	15.3	13.9	8.82	6.46
0.65	0.15	0.16	0.16	0.15	1.60	1.13	1.70	1.63	2.11	2.15	2.46	2.22	2.29	4.56	3.37	2.60	2.33	4.80	11.9	10.4	6.87	5.17
1.03	0.12	0.13	0.12	0.12	0.83	0.58	0.89	0.85	1.59	1.10	1.69	1.63	2.26	2.99	2.82	2.43	2.28	3.07	7.5	5.53	4.01	3.22
1.40	0.11	0.11	0.12	0.11	0.50	0.40	0.54	0.51	1.06	0.70	1.12	1.08	2.18	1.98	2.41	2.27	2.19	2.62	6.3	4.2	3.23	2.71
2.40	0.11	0.11	0.11	0.11	0.23	0.22	0.25	0.23	0.44	0.35	0.48	0.44	1.48	0.88	1.53	1.51	1.48	–	4.91	3.9	3.66	3.22

The analysis of calculational results has shown that the effects of inhomogeneity of the particle structures (double–layer) are at the level of measurement errors for the extinction coefficients σ_{ext} in the model *A*. For example, the relative error of σ_{ext} is 0.1–2% for very large particles.

For the model *B* the replacement of water–soot particles by homogeneous water or soot particles results in great variations, and only for large particles with the soot cover, which is 1 and 10% in mass, one can neglect the effect of the water core and consider them as pure soot particles. It should be noted that in the case of the radiation extinction by small particles their layered structure shows stronger influence.

The particle inhomogeneity more strongly effects on the absorption characteristics. We have considered a ratio of the absorption coefficients for the models of double–layer and homogeneous particles as a criterion of such an effect (Tables II and III) $K_{abs}=\sigma_{abs}$(double–layer)/σ_{abs}(homogeneous).

Significant decrease of the value *K* down to 0.03–0.2 is observed for the model *A* in the case of thin shields due to the replacement of double–layer particles by the homogeneous ones with the "effective" complex refractive index. The variation of K_{abs} is insignificant (~ 0.8–1.2) for the fine fraction in the case of thick shields (10 % of soot), while for the coarse fraction of aerosols K_{abs} exceeds unity. For example, for mode V K_{abs} is equal to 3.39 at the wavelength λ = 1.4 μm.

For the model *B* the replacement of the double–layer water–soot particles by the homogeneous soot ones results in a K_{abs} decrease which depends on the shield thickness and the diffraction parameter $\rho = 2\pi r/\lambda$; with K_{abs} being below unity everywhere over the spectrum.

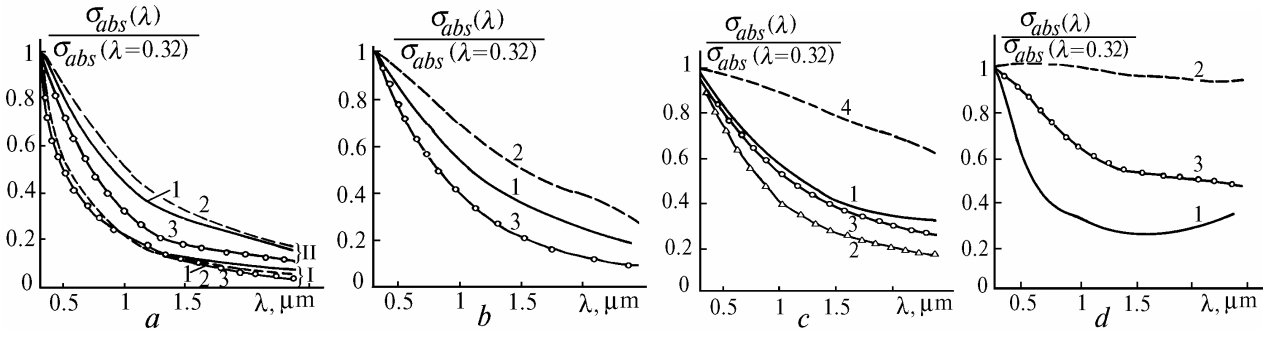

FIG. 1. Relative spectral behavior of the absorption $K_{abs} = \sigma_{abs}(\lambda)/\sigma_{abs}$ (λ = 0.32 μm) *for the model A: a and b) Modes I, II, and III, c) Mode IV, and d) Mode V (curves 1 are for homogeneous particles with the "effective" complex refractive index* $\tilde{m} = (\tilde{n} - i\tilde{k})$ *and curves 2, 3, and 4 are for double–layer particles with the soot cover,* 10, 1, *and* 0.1 %, $m_c = (\tilde{n} - i0)$, $m_{sh} = m_{soot}$ *).*

The spectral behavior of the normalized absorption coefficient $\sigma^n_{abs}(\lambda) = \sigma_{abs}(\lambda)/\sigma_{abs}(\lambda = 0.32\ \mu m)$ is shown for the model *A* in Fig. 1 and for the model *B* in Fig. 2. The monotonic decrease of $\sigma^n_{abs}(\lambda)$ with increasing λ is observed in the entire wavelength range under consideration for the model *A*. For the model *B* the increase of $\sigma^n_{abs}(\lambda)$ with increasing λ is caused by the spectral dependence of the soot absorption coefficient. The step–wise increase at λ = 1 μm is explained by the effect of the water absorption coefficient. The spectral dependence of the energy scattering characteristics makes it impossible to judge on the size and type of scattering particles. In order to correctly estimate the energy characteristics of the scattering medium, it is necessary to know the particle type (size, inner structure, and optical constants).

Certain conclusions on the type of particles can be drawn from the analysis of angular characteristics of scattering we have considered above, with the polarization characteristics of scattering being most important. The intensity of scattered radiation $I(\theta)/I(0°)$ at λ = 0.55 μm is shown for the model *A* in Fig. 3 and for the model *B* in Fig. 4.

The dimensionless intensity for the small scattering angles ($\theta < 60°$) depends mainly on the diffraction parameter, but the dependence on the value of the complex refractive index m and the inner structure becomes essential with the scattering angle increase, i.e., the asymmetry of scattering appears. The angular behavior of the intensity of scattering becomes more complicated, i.e., the additional scattering minima appear in the range of large scattering angles. The first minimum appears in the range of $\theta = 120–130°$ for the considered models, and the second minimum appears in the range of $\theta = 160–170°$ depending on the refractive index. Gorshkova et al. and Smerkalov[7,8] attempted to derive the analytical expressions relating the particle refractive index with the parameters of the particle size distribution and with the asymmetry coefficient of the scattering phase function

$$\Gamma = \frac{\int_{0}^{\pi/2} I(\Theta) \sin\Theta \, d\Theta}{\int_{\pi/2}^{\pi} I(\Theta) \sin\Theta \, d\Theta} .$$

These analytical expressions, however, do not take into account the inner particle structure.

The degree of linear polarization $P(\theta)$ at $\lambda = 0.55$ μm is presented for the model B in Fig. 5 and for the model A in Fig. 6.

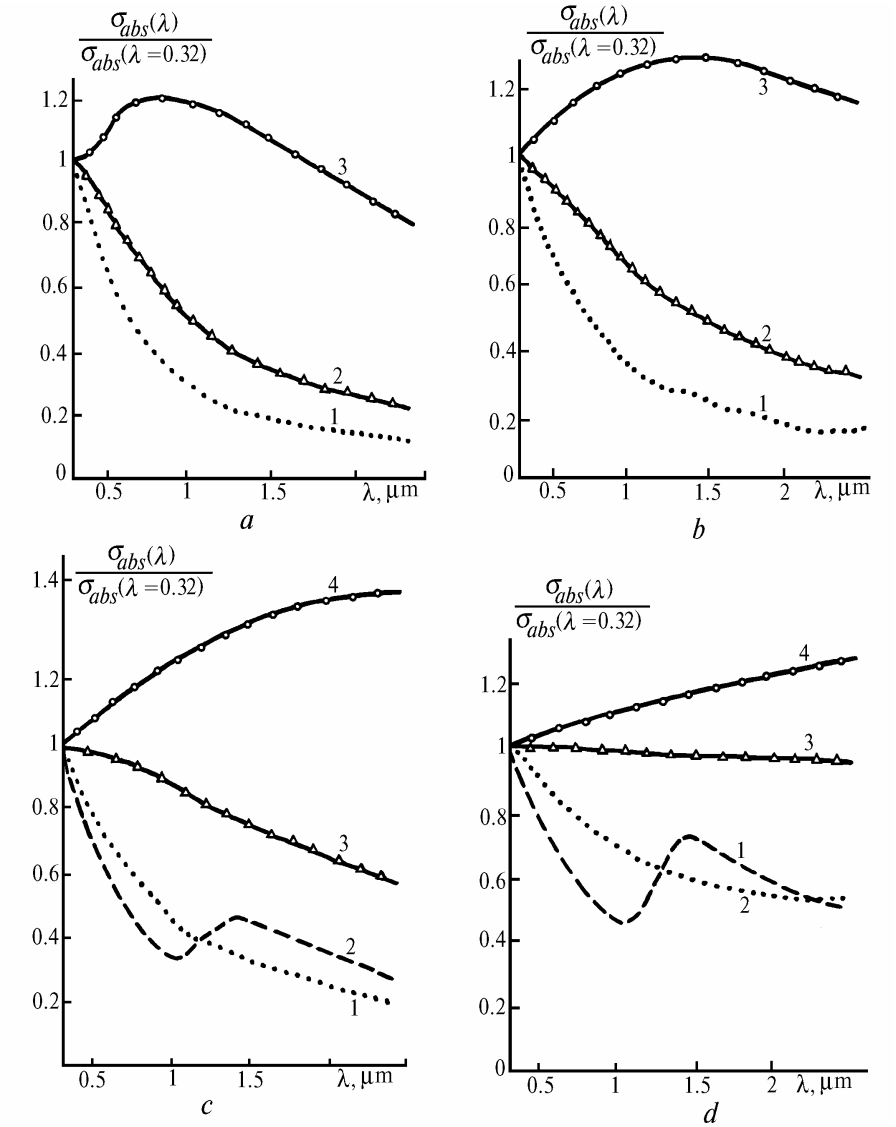

FIG. 2. Relative spectral behavior of the absorption $K_{abs} = \sigma_{abs}(\lambda)/\sigma_{abs}(\lambda = 0.32\ \mu m)$ *for the model B: a and b) Modes I and II (curves 1 and 2 are for double–layer particles with the soot cover* 1 *and* 10 %, *the complex refractive index* $m_c = m_{water}$, $m_{sh} = m_{soot}$*) and c, d) Modes IV and V (curves 1, 2, and 3 are for double–layer particles with the soot cover* 0.1, 1, *and* 10 %, $m_c = m_{water}$, *and* $m_{sh} = m_{soot}$ *and curves 4 are for homogeneous particles with* $m = m_{soot}$*).*

As can be seen from these figures, Mode I (models A and B) corresponds to a pure Rayleigh scattering. Neither the inner structure of the particles nor the complex refractive index effect on the curve shapes. With increase of particle size the scattering asymmetry increases and the maximum polarization shifts to the side angles (in the range

of $\theta < 90°$ for soot), there also appear a negative polarization and additional maxima. The maxima are specifically characteristic of a concrete substance with certain inner structure.

Thus, the results of the analysis of the data of numerical modeling for different models of the atmospheric aerosol microstructure show that the angular characteristics, especially the degree of linear polarization, are most sensitive to the microstructure variations. The effect of the microstructure variations on these characteristics greatly exceeds the measurement errors, and, therefore, can be used for observations of the condensation processes in aerosols and clouds. The effect of the soot cover is especially strong, it is determined both by the size of the double–layer particles and by the thickness of a soot shield. In the case of very small particles the variations of the degree of the linear polarization and the scattering phase function are practically equal for the particles of any composition (Rayleigh scattering). For the other modes the character of $I(\theta)$ and $P(\theta)$ is determined mainly by the thickness of the soot shield and to a certain degree depends on the chemical composition of the core (i.e., on κ of the core substance).

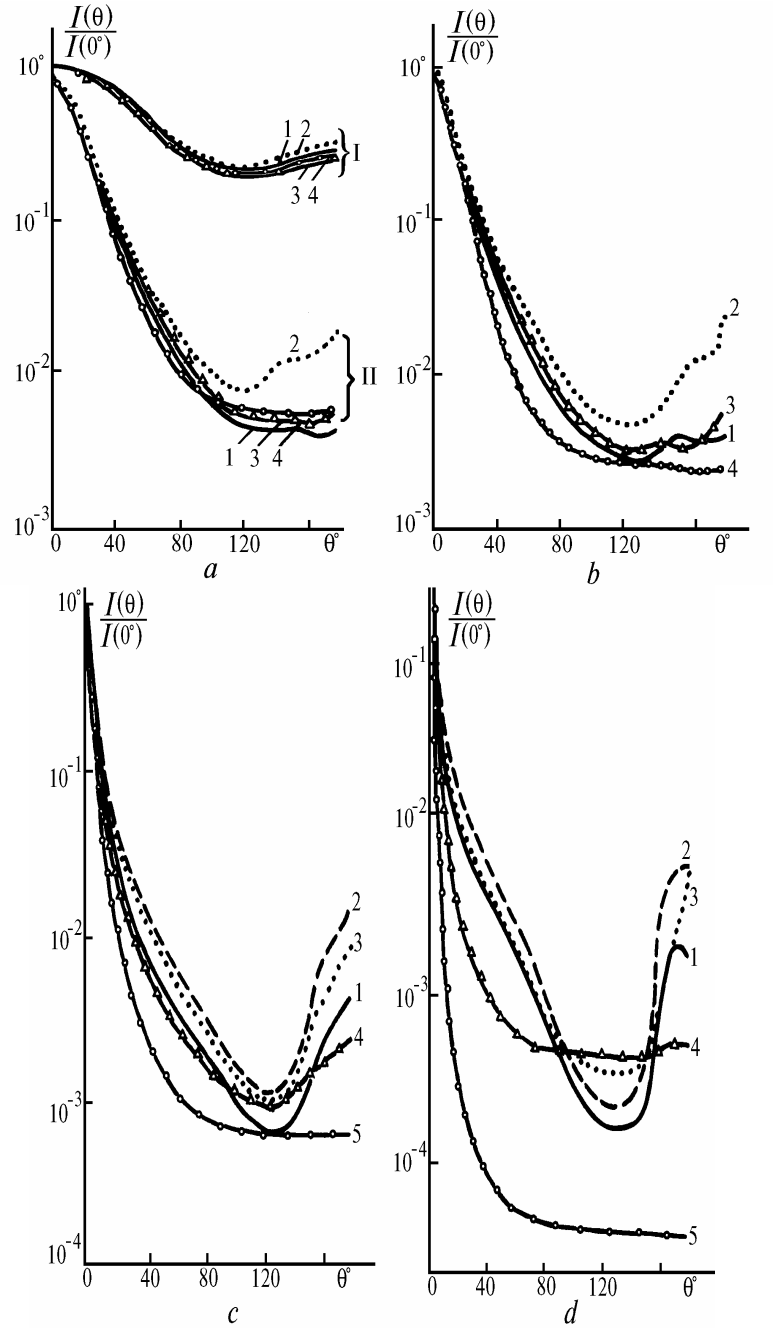

FIG. 3. Scattering phase functions $I(\theta)/I(0°)$ at $\lambda = 0.55$ μm for the model A: a and b) Modes I, II, and III (curves 1 are for homogeneous particles with "effective" complex refractive index $\tilde{m} = (\tilde{n} - i\tilde{k})$; curves 2 and 3 are for double–layer particles with the soot cover 1 and 10 %; $m_c = (\tilde{n} - i{\cdot}0)$ and $m_{sh} = m_{soot}$); c and d) Modes IV and V (curves 1 are for homogeneous particles with $\tilde{m} = (\tilde{n} - i\tilde{k})$; curves 2, 3, and 4 are for double–layer particles with the soot cover 0.1, 1, and 10 %, $m_c = (\tilde{n} - i{\cdot}0)$, and $m_{sh} = m_{soot}$; and, curve 5) is for homogeneous particles with $m = m_{soot}$).

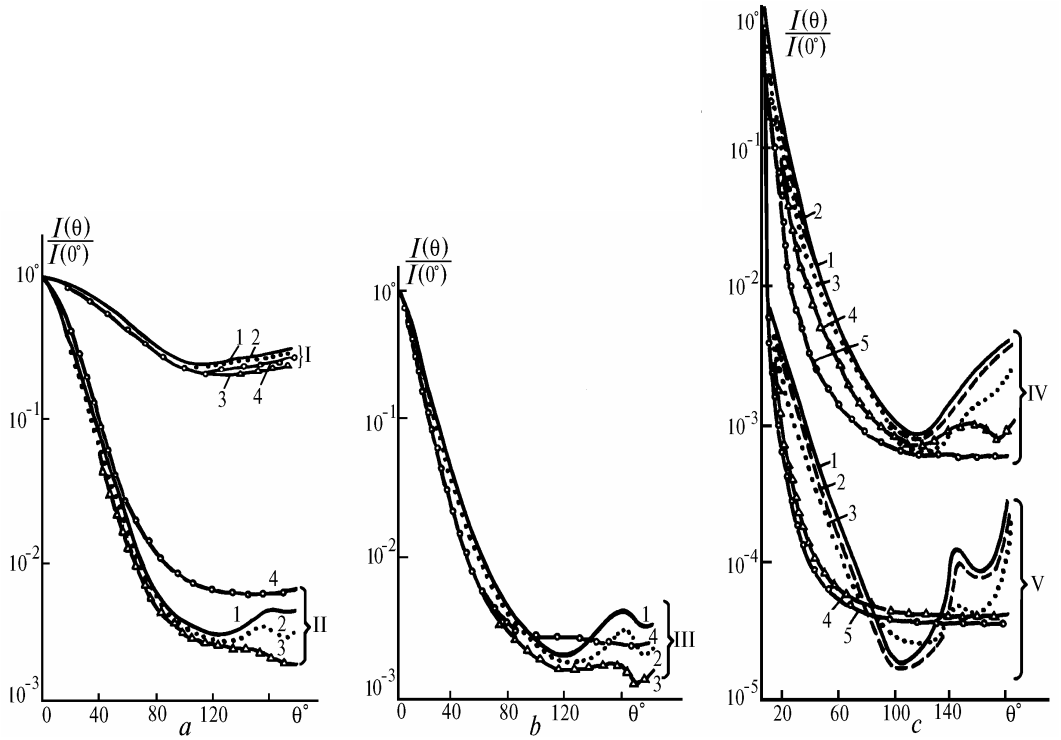

FIG. 4. Scattering phase functions $I(\theta)/I(0°)$ at $\lambda = 0.55$ μm for the model B: a and b) Modes I, II, and III (curves 1 are for homogeneous particles with complex refractive index $m = m_{water}$; 2 and 3 are for double–layer particles with the soot cover 1 *and* 10 %, $m_c = m_{water}$, *and* $m_{sh} = m_{soot}$, *curves 4 are for homogeneous particles* $m = m_{soot}$), *and c) Modes IV and V (curves 1 are for homogeneous particles with* $m = m_{water}$, *2, 3, and 4 are for double–layer particles with the soot cover* 0.1, 1, *and* 10 %, $m_c = m_{water}$, *and* $m_{sh} = m_{soot}$; *and, curve 5 is for homogeneous particles with* $m = m_{soot}$).

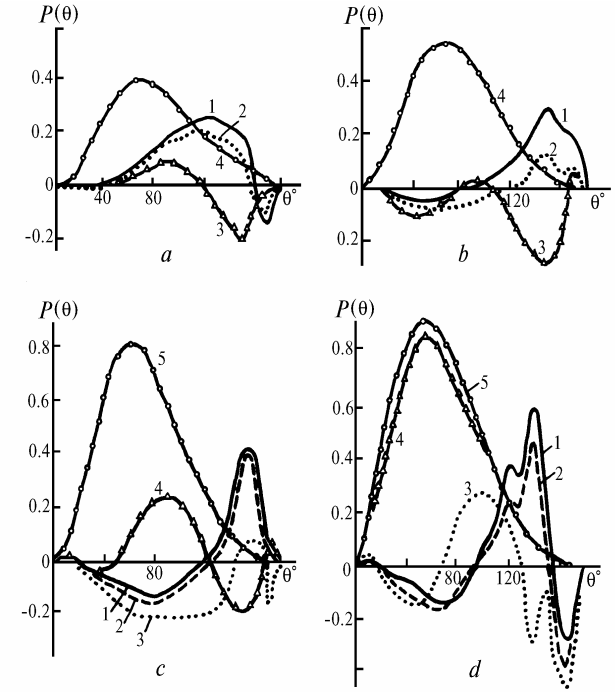

FIG. 5. Degree of linear polarization of the scattered radiation $P(\theta)$ *at* $\lambda = 0.55$ μm *for the model A: a) Modes I and II; b) Mode III (curves 1 are for homogeneous particles with "eefective" complex refractive index* $\tilde{m}=(\tilde{n}-i\cdot\tilde{k})$; *curves 2 and 3 are for double–layer particles with the soot cover* 1 *and* 10%, $m_c=(\tilde{n}-i\cdot 0)$, *and* $m_{sh}=m_{soot}$; *curves 4 are for homogeneous particles with* $m=m_{soot}$), *c and d) Modes IV and V (curves 1 are for homogeneous particles with* $m=\tilde{m}$; *curves 2,3,and 4 are for double–layer particles with the soot cover* 0.1, 1, *and* 10%, $m_c=(\tilde{n}-i\cdot 0)$ *and* $m_{sh}=m_{soot}$; *and, curve 5 is for homogeneous particles with* $m=m_{soot}$).

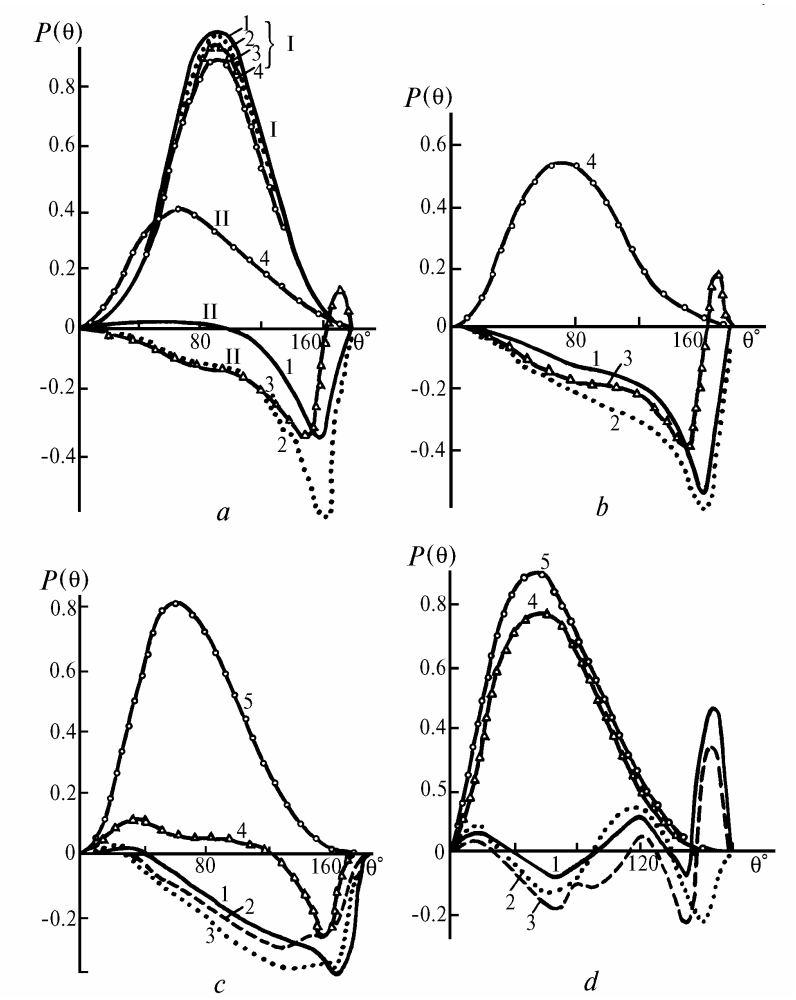

FIG. 6. Degree of linear polarization of the scattered radiation P(θ) at λ = 0.55 μm for the model B: a) and b) Modes II and III (curves 1 are for homogeneous particles with m = m_{water}; curves 2 and 3 are for double–layer particles with the soot cover 1 *and* 10%, $m_c = m_{water}$ *and* $m_{sh} = m_{soot}$; *curves 4 are for homogeneous particles with* $m = m_{soot}$); *c and d) Modes IV and V (curves 1 are for homogeneous particles with* $m = m_{water}$; *curves 2, 3, and 4 are for double–layer particles with the soot cover* 0.1, 1, *and* 10%, $m_c = m_{water}$, *and* $m_{sh} = m_{soot}$; *and, curve 5 is for homogeneous particles with* $m = m_{soot}$).

REFERENCES

1. A.P. Prishivalko and L.G. Astaf'eva, "*Absorption, scattering and extinction of light by the atmospheric aerosol particles, covered with water*", Preprint, Inst. of Physics, Academy of Sciences of Belarus, Minsk (1975).
2. A.P. Prishivalko, V.A. Babenko, and S.T. Leiko, Opt. Spektrosk. **29**, No. 1, 162–169 (1975).
3. C.F. Bohren and D.R. Huffman, *Absorption and Scattering of Light by Spherical Particles* (John Wiley and Sons, New York–London, 1983).
4. B.J. Meison, *Cloud Physics* (Gidrometeoizdat, Leningrad, 1961), 542 pp.
5. K.Ya. Kondrat'ev, V.I. Binenko, and O.P. Petrenchuk, Izv. Akad. Nauk SSSR, Fiz. Atmos. Okeana **17**, No. 2, 167–174 (1981).
6. L.S. Ivlev, *Chemical Composition and Structure of Atmospheric Aerosols* (Leningrad State University Press, Leningrad, 1982).
7. N.I. Gorshkova, O.M. Korostina, and V.A. Smerkalov, Atm. Opt. **3**, No. 3, 214–218 (1990).
8. V.A. Smerkalov, Issled. Zemli iz Kosmosa, No. 3, 8–13 (1991).